Comparison of Steady-State Characteristics between DFIG and SCIG in Wind Turbine

Phan Dinh Chung

Electrical Engineering Department,
Danang University of Technology, Vietnam
chungpy99d6@yahoo.com

Abstract

Variable speed wind turbine with doubly-fed induction generator (DFIG) is gradually replacing fixed speed one with squirrel cage induction generator (SCIG) in wind power applications. It is worthwhile to compare these two generators with respect to operating principle, controlling ability, etc. This paper concentrates on analyzing active/reactive power relationship in steady-state between DFIG and SCIG by simulation on MATLAB. Another key task investigated in this paper is comparison of electromechanical torque-slip characteristics between DFIG and SCIG with several different conditions such as interconnecting network strength and type, generator terminal voltage, and rotor resistance. Comparison results verify that DFIG has distinct features over SCIG.

Keywords: *Wind turbine; active/reactive power; DFIG; SCIG; torque-slip characteristic*

1. Introduction

Emission from fossil fuels and their depletion have risen in an awareness of searching for alternative energy resources and renewable energy applications are becoming an interesting topic in the world. In particular, wind energy has been one of the most popular subjects in recent research and development. Fixed speed wind turbine equipped with SCIG has the advantages of being simple, robust and reliable. However, it also contains some disadvantages of uncontrollable reactive power output, mechanical stress and limited power quality control. Owing to its fixed speed operation, fluctuations in wind speed are further transmitted as fluctuations in the mechanical torque and then in the electrical power output [1]. In order to overcome the above mentioned problems associated with fixed-speed wind turbine system and to maximize the wind energy capture, variable speed wind turbines based on DFIG are becoming employed. Differences come from such categories as speed control, reduced flicker, and four-quadrant active and reactive power capabilities.

Both DFIG and SCIG are classified as induction machine but there is a little difference in their rotor sides. This leads to many differences in steady-state electrical characteristics, mechanical curves and dynamic responses when connected to the grid. A study concerning methodologies of speed control of DFIG to produce electrical energy on network is given in [2], where PI and RST controller are feasibly used to control active and reactive power exchange between DFIG and network. Impacts of AC/DC/AC converter on the steady-state characteristics of DFIG were also studied by the researchers in [3-5]. The authors analyzed the output of DFIG as changing d-q components of rotor voltage based on the d-q frame in order to compare active powers in the rotor side and the stator side. In reference [6], the author calculated steady-state operation for DFIG, where a method based on the Newton-Raphson algorithm is proposed for obtaining the steady-state electrical characteristics of the machine under various conditions. The relationship between active power and angle of rotor

voltage at some specific rotor slip is considered in [7]. The superposition principle is applied and the torque production is viewed as the summation of effects of the stator excitation. Likely, the effects of converter on power and torque characteristics were investigated in [8].

Some researchers focused on assessing the capability of reactive power provision of DFIG to the grid. They evaluated ability and limitation of reactive power caused by the power restriction of the converter connected in the rotor side. The P-Q relationship in some specific conditions is shown in [9, 10] and the dynamic and transient characteristics of DFIG were reported precisely in [11, 12]. Comparison between DFIG and traditional induction generator are made in different cases [13]. The modeling and controlling strategies of fixed speed and doubly-fed asynchronous generator were described and compared during power system disturbances. However, the power flow in DFIG has not been performed visibly and the disparity in torque-slip curve between DFIG and SCIG has not been investigated.

To provide a comparison of steady-state characteristics between DFIG and SCIG, this paper focuses on investigating the active and reactive power outputs of stator and rotor sides for each generator with respect to rotor slip variations and, in addition, conducting an examination of P-Q relationship at the rated operating points by simulation in Matlab. Another task done in this paper is the comparison between DFIG and SCIG in electromechanical torque-slip characteristics with respect to changing interconnecting network strength and type, generator terminal voltage, and rotor resistance of the generator to draw out distinct features of DFIG.

2. Comparison of Output Power between DFIG and SCIG

2.1. Equivalent Circuit of DFIG

A doubly fed induction generator is basically a wound rotor induction generator fed by both stator and rotor, as can be seen in Figure 1, in which the stator winding is directly connected to the grid and the rotor winding is connected to the grid through AC/DC/AC converters. These converters are divided into two components: the rotor side converter and the grid side converter. A capacitor between the converters plays a role of a DC voltage source. A coupling inductor is used to link the grid side converter to the grid.
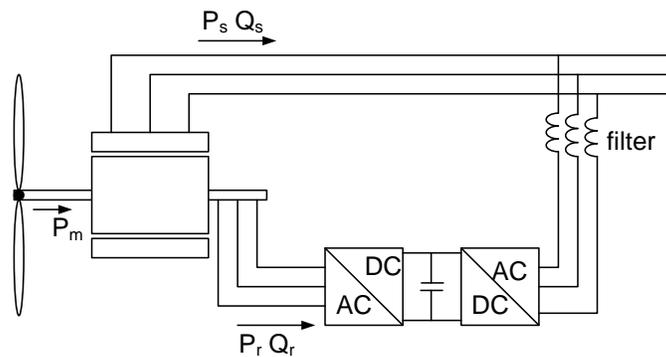

Figure 1. Configuration of DFIG based Wind Turbine

The operation principle of DFIG is fundamentally the same as that of a transformer. Thus, DFIG can be represented as a transformer's per phase equivalent circuit, where R_r and X_r represent rotor resistance and reactance referred to the stator side. But the equivalent circuit

of induction machine differs from a transformer's primarily with respect to varying rotor frequency on the rotor voltage. In case of DFIG, there is a voltage injected to the rotor winding, so an equivalent circuit of classic induction machine needs to be modified by adding a rotor injected voltage as shown in Figure 2. In this figure, s is the rotor slip, V the voltage, I the current, R and X represent resistance and reactance, respectively. The subscripts r, s and m stand for rotor, stator and mutual, respectively.

Real and reactive power in the stator side, P_s, Q_s, delivered to the connected grid can be derived from I_s and V_s, as in (1).
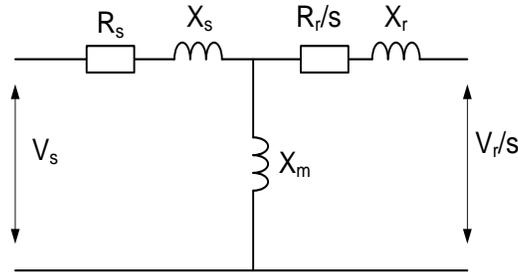

Figure 2. The Equivalent Circuit of DFIG

$$P_s = 3\mathrm{Re}(V_s I^*_s) \tag{1}$$
$$Q_s = 3\mathrm{Im}(V_s I^*_s)$$

Real and reactive power in the rotor side, P_r, Q_r, referred to stator side is derived from I_r and V_r/s, as in (2).

$$P_r = 3\mathrm{Re}(\frac{V_r}{s} I^*_r) \tag{2}$$
$$Q_r = 3\mathrm{Im}(\frac{V_r}{s} I^*_r)$$

It is possible to express the electromechanical torque, T_e, as in (3).

$$Te = \frac{3}{2}\frac{p}{2}\mathrm{Re}(j\Psi_s I^*_s) = \frac{3}{2}\frac{p}{2}\mathrm{Re}(j\Psi_r I^*_r) \tag{3}$$

Where

$$\Psi_s = \frac{X_s I_s + X_m I_r}{\omega_s}; \quad \Psi_r = \frac{X_r I_r + X_m I_s}{\omega_s} \tag{4}$$

Ψ_s and Ψ_r: the stator and the rotor flux, respectively.

p: the number of poles per phase.

I^*_s, I^*_r: the complex conjugates of the stator and the rotor current, respectively.

2.2. Active Power between DFIG and SCIG

When DFIG is used as a generator in wind turbine, the power output depends not only on mechanical power input transmitted by the shaft of wind turbine but also on the behavior of AC/DC/AC converter connected between the rotor winding and the grid. A simulation on Matlab is implemented with parameters listed in the Table 1 in order to analyze the power output in DFIG.

Table 1. Parameters of DFIG for Simulation

Rated power	1.5 MW
Rated voltage	0.69 kV
Stator resistance R_s	0.00706 pu
Rotor resistance R_r	0.005 pu
Stator inductance L_s	0.171 pu
Rotor inductance L_r	0.156 pu
Mutual inductance L_m	2.9 pu

A traditional induction generator (SCIG) generally exchanges energy with the interconnected grid via only the stator winding while the rotor winding is short-circuited. In DFIG, energy can be exchanged with the linked network by not only the stator winding but also the rotor winding. Moreover, the machine side converter can conveniently control the power flow to the grid.
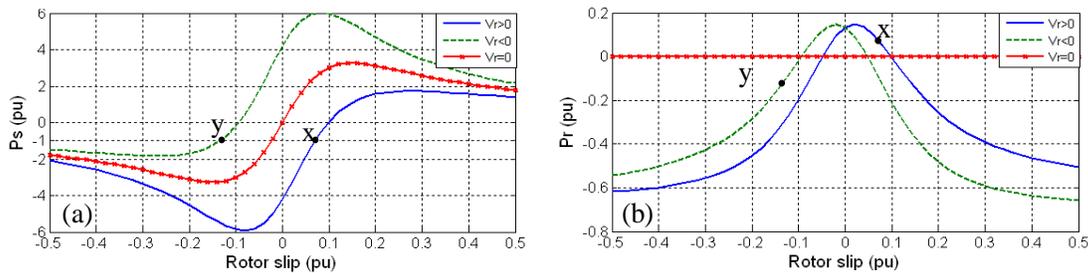

Figure 3. Active Power Output of DFIG for the Stator Side (a), and the Rotor Side (b)

A vast proportion of active power that DFIG exchanges with the interconnected grid comes from the stator winding but this active power output also depends on the rotor speed and the rotor voltage (V_r). Figure 3 (a) and (b) illustrate the stator active power (P_s) and rotor active power (P_r) of DFIG with respect to varying rotor side voltage, with SCIG's that corresponds to the V_r=0 curve. The points 'x' and 'y' represent the rated operating points of DFIG for the sub-synchronous and super-synchronous modes, respectively.

As can be seen from Figure 3 (a), SCIG only supplies active power to the linked grid when rotor speed is over synchronous speed. Unlike SCIG, the stator winding of DFIG can deliver active power to the connected grid in sub-synchronous region if a positive voltage is applied to rotor winding. For SCIG, an increase in rotor speed leads to a rise of stator active power

but for DFIG, same active power can be produced at different rotor speeds by controlling rotor voltage.

One superior feature of DFIG compared with SCIG is that the rotor winding is connected to the system via AC/DC/AC converter while in SCIG, it is shorted. Therefore, active power in the rotor side of SCIG is always equal to zero whereas the rotor winding in DFIG contributes to the additional energy exchange between DFIG and grid. This energy exchange is almost directly proportional to the product of minus rotor slip (s) and active power in the stator side ($P_r=-sP_s$). In generating mode, rotor winding supplies active power to the connected grid for $V_r<0$ and power flow is reversed for $V_r>0$. This is resulted from change in the sign of rotor slip. From Figure3, the 'x' and 'y' points have the same sign in the stator power curves while in the rotor power curves, the points are located in opposite sign. Then the total power for the point 'x' is less than 1pu and that for the point 'y' is more than 1pu. This means that operating at the point 'y' provides more energy than at the point 'x'.

2.3. Reactive Power between DFIG and SCIG

Figure 4 (a) and (b) illustrate the stator reactive power (Q_s) and rotor reactive power (Q_r) of DFIG with respect to varying rotor side voltage, where the angle (δ) between V_s and V_r from the rotor side converter is set to 2°. The points 'x' and 'y' represent the rated operating points of DFIG for the sub-synchronous and super-synchronous modes, respectively, which are the same as those in Figure 3. In SCIG, to create magnetizing flux in generator, it must receive reactive power from the interconnected grid and it requires a higher reactive power to produce a higher active power, which are shown in $V_r=0$ curve in Figure 4 (a). Contrarily, the magnetizing flux in generator can be generated by stator or rotor winding in DFIG. Therefore, DFIG can absorb reactive power in the rotor or stator side depending on the behavior of converter.
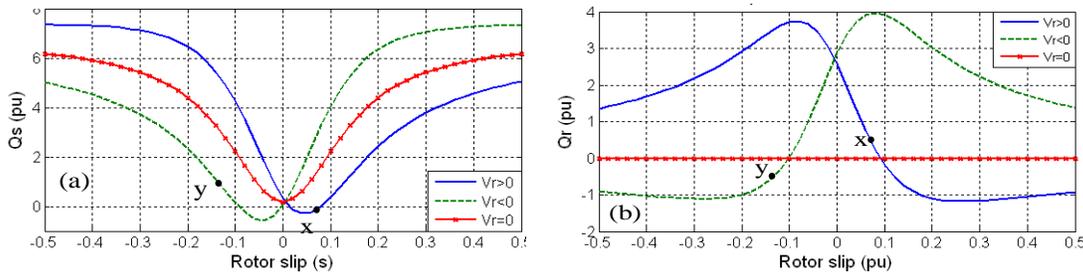

Figure 4. Reactive Power Output of DFIG for the Stator Side (a), and the Rotor Side (b) as Angle $\delta=2^o$

Since rotor winding is short-circuited, reactive power in the rotor side of SCIG is equal to zero as shown in $V_r=0$ curve in Figure 4 (b). However, the rotor winding of DFIG can absorb reactive power from the grid or supply a part of reactive power to the grid. The figure reveals that the rotor winding can compensate reactive power exchanged by the stator side to the grid.

Another thing drawn from Figure 4 is that reactive power at point 'y' absorbed by the stator side is much higher than that delivered by the rotor side. By contrast, reactive power at point 'x' absorbed by the rotor side is much higher than that supplied by the stator side. The reactive power output in the rotor side is completely opposite to that in the stator side for the rated generating mode. Therefore, DFIG can magnetize either the stator winding or the rotor winding and total reactive power absorbed from the grid is less than that in SCIG.

By similar simulations with different δ angles, an interesting thing for reactive power output can be absorbed with the angle variation. Figure 5 (a) and (b) illustrate the stator reactive power and rotor reactive power of DFIG with respect to varying rotor side voltage, where the angle (δ) between V_s and V_r from the rotor side converter is set to 20°. By comparing those with Figure 4, the 'x' and 'y' points are shifted in the opposite positions from the horizontal axis. It means that reactive power of DFIG can be absorbed from or delivered to the grid by controlling the δ angle between V_s and V_r from the rotor side converter. Therefore, reactive power output of DFIG heavily depends on the mechanical power input, the magnitude of V_r and the δ angle. This indicates that by cooperating with a reasonable control of a rotor-side converter, the reactive power output in rotor side of DFIG can be maintained in spite of a change in mechanical power.
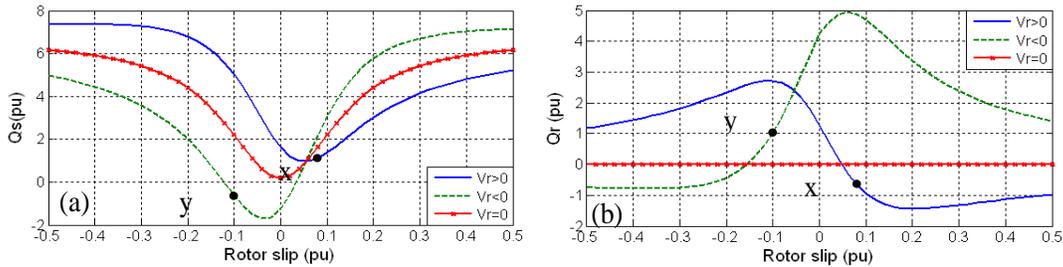

Figure 5. Reactive Power Output of DFIG for the Stator Side (a), and the Rotor Side (b) as Angle δ=20°

2.4. P-Q Relationship between DFIG and SCIG

Figure 6 illustrates the relationship between active power and reactive power in DFIG for the stator side, rotor side and total values, respectively, where the point 'z' represents the rated operating point of SCIG. To capture a specific active power, a reactive power output exchanged from the grid may be different depending on the behavior of converter, which means that the power factor of wind power plant using DFIG can be easily adjusted. As can be seen from Figure 6 (a) and (b), the locus of the rated power operating point is the line connected between the point 'x' and 'y'. However, in Figure 6 (c), the performance of P-Q curve in total power, which is sum of stator and rotor powers, indicates that the locus of the rated power generating point is not a straight line. This locus consists of two lines, z-x and z-y for V_r>0 and V_r<0, respectively. This is resulted from rotor active power being opposite to that in the stator for the case of V_r>0. A reduction in V_r leads to a decline of absorbed power in the rotor side while in the stator side, the demand of reactive power is higher to create a flux compensating for decrease in the rotor winding flux. As a result, exchange of active and reactive power for the grid increases when the magnitude of V_r decreases. On contrary, for V_r<0 case, a decrease in the magnitude of V_r leads to a decline of active power delivered from the rotor winding. At the same time, reactive power extracted from the rotor winding is reduced so it requires the decrease in reactive power absorbed by the stator winding. As a consequence, total reactive power is reduced with reduction of total active power. When V_r reaches to zero, DFIG becomes SCIG, so the rated power generating point approaches to the point 'z', 1pu.
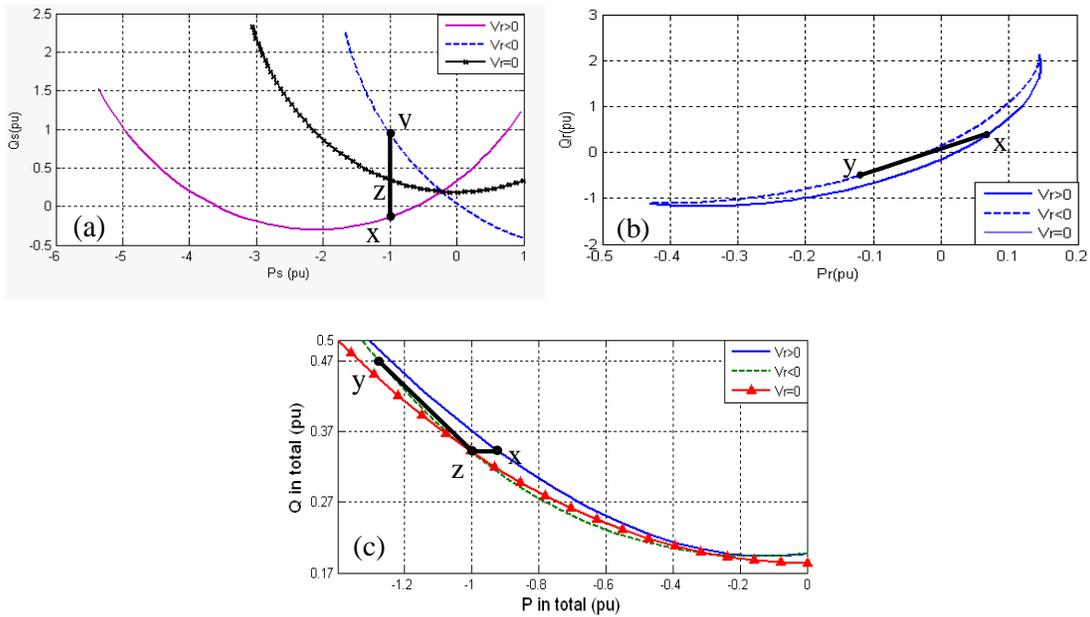
Figure 6. P-Q Relationship of DFIG for the Stator Side (a), the Rotor Side (b), and Total Power (c)

3. Electromechanical Torque-slip Characteristics between SCIG and DFIG

To assess strong features of DFIG compared with SCIG, the steady-state electromechanical torque-slip characteristics are drawn. Let us assume a simple model including the DFIG connected to a grid. The equivalent circuit illustrated in Figure 7 is formed to investigate the characteristics by simulating based on MATLAB. In this figure, V_b is the voltage of the grid, X_{PFC} is the reactance of capacitor bank used for power factor correction, R_N and X_N are the resistance and reactance of the interconnecting network, respectively. DFIG used for this simulation has the same parameters listed in Table 1 above.
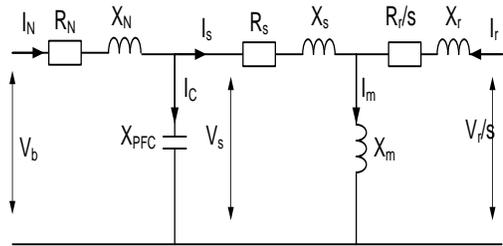

Figure 7. Equivalent Circuit of DFIG Interconnected to the Grid

The electromechanical torque-slip characteristics of DFIG compared with SCIG are different, depending on the parameters change of the interconnected wind turbine system. Several simulations are performed and results are summarized for the conditions such as strong or weak interconnecting network, overhead line or underground cable, the terminal voltage change and the rotor winding resistance change.

3.1. Strong or Weak Interconnecting Network

Figure 8 (a) and (b) illustrate the torque-slip characteristics of SCIG and DFIG with respect to strong or weak interconnecting network. Regardless of being interconnected to a strong or weak network, the overall behavior of DFIG is essentially same as that of SCIG. From the figure the rotor speed at which the induction machine reaches its maximum torque when connected to strong network is higher than when connected to weak network since strong network has less interconnecting impedance.
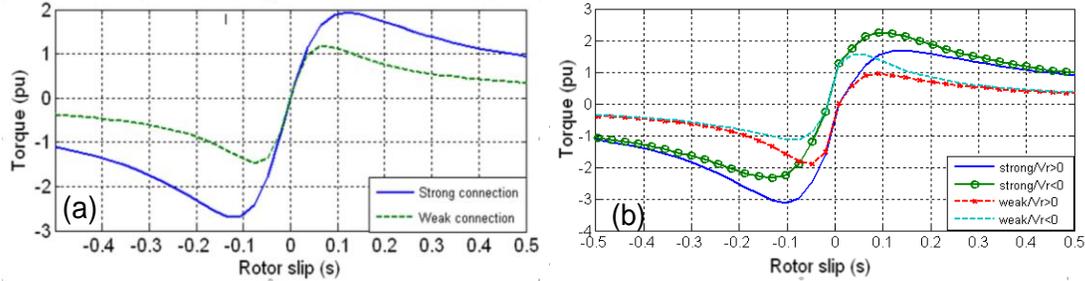

Figure 8. Torque-slip Characteristics of SCIG (a) and DFIG (b) as Connected to Strong or Weak Grid

However, depending on the supplied rotor voltage, DFIG performs differently from SCIG. With the same rotor slip, DFIG can produce a higher torque than SCIG for the case of $V_r>0$ and this is reversed when a negative rotor voltage is fed. A key dissimilarity between DFIG and SCIG is that the sign change of the torque in DFIG happens in sub-synchronous region or super-synchronous region for $V_r>0$ or $V_r<0$, respectively, while this is equal to synchronous speed in SCIG. Clearly, in order to adjust the rotor speed, electromechanical torque can be easily changed by changing the sign of rotor voltage. Likewise, a deviation of mechanical torque input in SCIG can lead a significant change in the rotor speed whereas for DFIG, by adapting rotor voltage, electromechanical torque can be accommodated to mechanical torque to keep the rotor speed in the stable region.
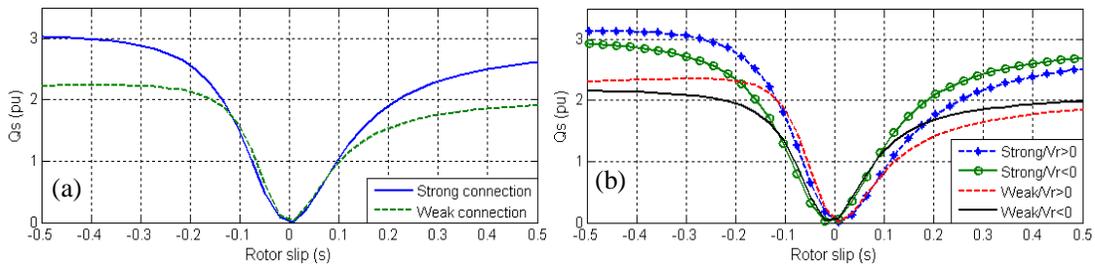

Figure 9. Reactive Power-slip Characteristics of SCIG (a) and DFIG (b) as Connected to Strong or Weak Grid

Figure 9 (a) and (b) show the reactive power-slip characteristics of SCIG and DFIG with respect to strong or weak interconnecting network. Reactive power for the strong network is higher than that for weak network in the range of larger rotor slip and reactive power for $V_r>0$ is less than that for $V_r<0$. With the range of rotor slip close to zero, there is an insignificant difference in reactive power curves between DFIG and SCIG.

From Figure 9 (a), as rotor slip is closed to zero, reactive power-slip curve of SCIG is steeper for weak grid case than that for strong one. For that reason, a small change in rotor speed leads to a big alteration of reactive power. This can cause a marked voltage variation on the grid especially in the case of a connected weak grid. Thus as SCIG connects to the grid, it often requires another equipment to support reactive power especially in the case of voltage sag on the grid or an interconnected weak grid. Unlike SCIG, the demand of reactive power of DFIG is not almost reliant on kinds of connected grid because torque curve is a wide area depending on rotor voltage. By varying rotor voltage, reactive power in the stator side can be retained despite of a change in rotor speed. Consequently, for DFIG, the oscillation of rotor speed can not affect voltage on the grid despite a linked weak grid. Additionally, for DFIG, by changing rotor voltage, it can meet easily the reactive power requirement of the grid code without any supportive equipment, even though a voltage dip occurs on the grid.

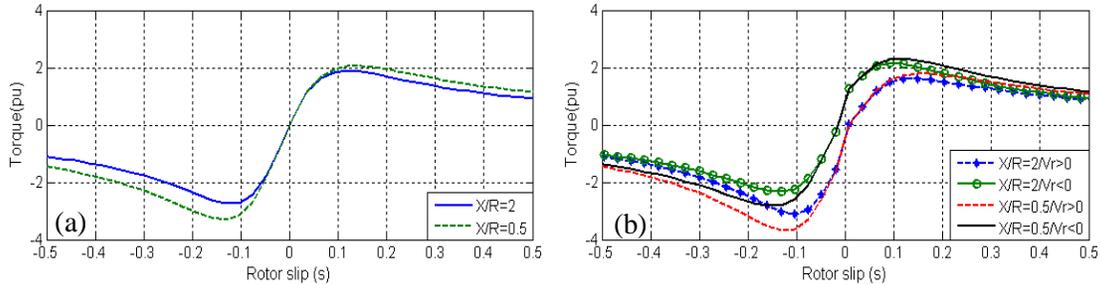### 3.2. Interconnecting Network with Overhead Line or Underground Cable

Figure 10. Torque-slip Characteristics of SCIG (a) and DFIG (b) being Connected to Overhead Line or Underground Cable

Figure 10 (a) and (b) illustrate the torque-slip characteristics of SCIG and DFIG with respect to overhead line or underground cable interconnecting network. Similar differences as the above clause are also seen when connected to overhead line (X/R=2) and underground cable (X/R=0.5).

As can be seen from Figure 10, DFIG exhibits a wide range of torque curve and it, thus, is less affected by the types of interconnecting network. Rotor slip of DFIG can vary in a quite wide range by accommodating rotor voltage to maintain torque output while for SCIG, a small change of rotor speed leads to a significant variation in torque output and this change is seen more clearly as SCIG is connected through underground cable.

3.3. Changing the Terminal Voltage

In some unexpected situation, the terminal voltage of generator would be dropped. This leads to a change in electromechanical torque of induction generator. Figure 11 (a) and (b) indicate the torque-slip characteristics of SCIG and DFIG as the generator terminal voltage (V_s) is equal to 100% or 80% of the normal value. From the figure the torque curve for the larger terminal voltage is higher than that for less terminal voltage.
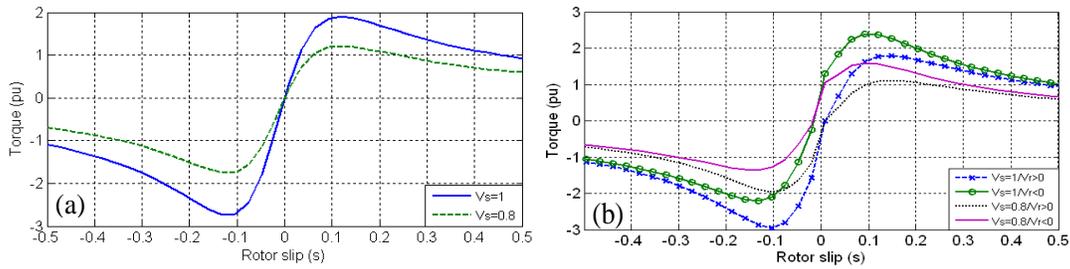
Figure 11. Torque-slip Characteristics of SCIG (a) and DFIG (b) for Stator Voltage Changes

For SCIG, a generator terminal voltage drop leads to a decrease in the maximum torque possible. It means that SCIG can be unstable if large voltage sag occurs. Figure 11 illustrates that the peak torque of DFIG is higher than that of SCIG when negative rotor voltage is applied and torque-slip curve of DFIG depends on both stator and rotor voltages. Consequently, the accommodation of rotor voltage makes DFIG be stable when a large decrease in stator voltage happens.

3.4. Changing the Resistance of Rotor Side

Figure 12 (a) and (b) illustrate the torque-slip characteristics of SCIG and DFIG as the rotor resistance (R_r) is equal to 0.3Ω or 0.7Ω. From the figure, the higher rotor resistance value the softer the electromechanical torque curve and thus change in rotor speed has less effect on variation of torque output.
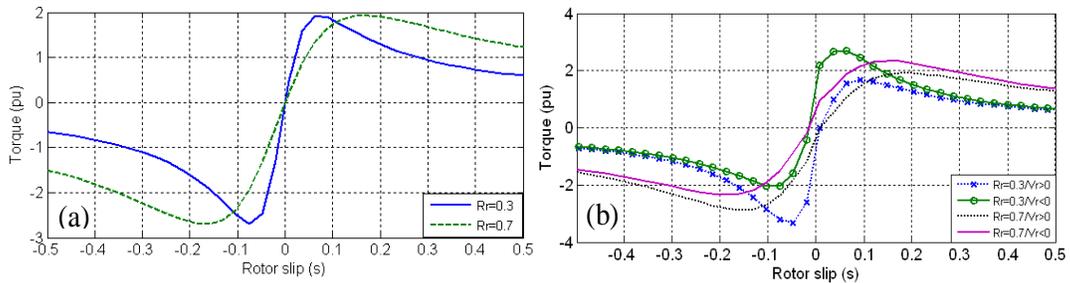

Figure 12. Torque–slip Characteristics of SCIG (a) and DFIG (b) for Rotor Resistance

In addition, in SCIG, this slope change does not affect the magnitude of pull-out torque but the pull-out torque varies with rotor resistance changes in DFIG. The less rotor resistance gives higher pull-out torque for the negative rotor voltage and an opposite thing happens for the positive rotor voltage.

4. Conclusion

This paper, by simulation on MATLAB, investigated the active and reactive power outputs of stator and rotor sides of both DFIG and SCIG with respect to rotor slip variations, and conducted an examination of P-Q relationship at the rated operating points for analysis of

steady-state characteristics between them. It also performed a comparison between DFIG and SCIG in electromechanical torque-slip characteristics with several different conditions.

Depending on the supplied rotor voltage (V_r), DFIG is able to generate active power as rotor speed is sub-synchronous or super-synchronous. In addition, reactive power in the stator and rotor winding of DFIG can be easily changed by adjusting the δ angle between Vs and V_r. Reactive power output of DFIG heavily depends on the mechanical power input, the magnitude of V_r and the δ angle. For the rated generating condition, total active power is higher in super-synchronous region than that in the sub-synchronous region.

The comparison of torque-slip characteristics between DFIG and SCIG is fulfilled with several different conditions and a few features are derived. The rotor speed at which the induction machine reaches its maximum torque when connected to strong network is higher than when connected to weak network. Similar differences are observed when connected to overhead line or underground cable. The rotor resistance change in SCIG does not affect the magnitude of pull-out torque but the pull-out torque varies with rotor resistance changes in DFIG. The less rotor resistance gives higher pull-out torque for the negative rotor and an opposite thing happens for the positive rotor voltage.

Thus, DFIG offers a wide range of torque-slip curve depending on the rotor voltage control. This allows DFIG to be able to operate with variable speed while SCIG needs to be operated in fixed speed.

References

[1] T. Ackerman, "Wind power in power system", Royal Institute of Technology Stockholm, Sweden **(2005)**.
[2] F. Poitiers, M. Machmoum, R. L. Doeuff and M. E. Zaim, "Control of a doubly-fed induction generator for wind energy conversion system", http://itee.uq.edu.au/~aupec/aupec01/026_%20POITIERS%20_ AUPEC01%20paper%20revised.pdf, **(2009)**.
[3] S. Li, T. A. Haskew and J. Jackson, Renew. Energy, vol. 35, **(2009)**, pp. 42.
[4] S. Li and S. Sinha, "A simulation analysis of double –fed induction generator for wind energy conversion using PSpice", Power Enginering Society General Meeting, IEEE, 10.1109/PES. 1708952, **(2006)**.
[5] S. Li, T. A. Haskew and J. Jackson, "Power generation characteristic study of integrated DFIG and its frequency converter", Power and Energy Society General Meeting - Conversion and Delivery of Electrical Energy in the 21st Century, IEEE, 10.1109/PES.2008.4596058, **(2008)**.
[6] J. F. M. Padrón and A. E. F. Lorenzo, IEEE Trans. Power Syst., vol. 25, **(2009)**, pp. 922.
[7] L. Jiao, B. T. Ooi, G. Joós and F. Zhou, Electr. Power Syst. Res., vol. 76, **(2005)**, pp. 33.
[8] B. B. Rajapalan, J. Electr. Eng., vol. 60, **(2009)**, pp. 79.
[9] Arulampalam, M. Barnes, N. Jenkins and J. B. Ekanayake, "Power quality and stability improvement of a wind farm using Statcom supported with hybrid battery energy store", IEE Proc.-Gener. Transm. Distrib., vol. 153, no. 6, **(2006)**.
[10] T. Lund, P. Sørensen and J. Eek, Wind Energ., vol. 10, **(2007)**, pp. 379.
[11] H. Jia-bing and H. Yi-kang, J. Zhejiang Univ. SCIENCE A. 7, **(2006)**, pp. 1757.
[12] B. C. Babu, K. B. Mohanty and C. Poongothai, "Wind Turbine Driven Doubly-Fed Induction Generator with Grid Disconnection", http://eeeic.eu/proc/papers/6.pdf.
[13] L. Holdsworth, X. G. Wu, J. B. Ekanayake and N. Jenkins, "Comparison of fixed speed and doubly fed induction wind turbines during power system disturbance", IEE Proceedings, Generation, Transmission and Distribution, vol. 150, **(2003)**, pp. 343–352.

Author

Phan Dinh Chung

He was born in Vietnam, 1980. He received B.Sc. Eng. degree from Danang University of Technology, Vietnam, in 2004 and M.Sc. Eng. degree from Dongguk University, Seoul, South Korea 2011, all in electrical engineering.

He has been working as a lecture in Danang University of Technology, Vietnam since 2004. His research interests include renewable energy, power conversion system, power quality, VSC-HVDC transmission system, and power system stability and micro-grid.